Quantum Electronics **33** (7) 568 – 580 (2003)

PACS numbers: 42.55.Lt; 42.60.Lh
DOI: 10.1070/QE2003v033n07ABEH002464

High-power pulsed dense-gas lasers

G.A. Mesyats, V.F. Tarasenko

***Abstract*. Research works on pulsed dense-gas lasers co-authored by A.M. Prokhorov are reviewed, and an analysis is made of the significance of this research for the subsequent development of high-power gas lasers. The emphasis is placed on the investigation of CO_2 lasers pumped with an e-beam-controlled discharge, an e-beam-pumped argon – nitrogen mixture laser, and also exciplex lasers utilising rare-gas halides.**

Keywords: *pulsed dense-gas lasers, CO_2 laser, exciplex lasers.*

1. Introduction

The progress of quantum electronics in the 1970s – 1980s is largely related to the advent and development of high-power pulsed lasers utilising dense gases pumped by an electron-beam-controlled discharge, a self-sustained discharge, and an electron beam. A.M. Prokhorov played a great role in the initiation and development of these investigations, and he was also a co-author of a large number of pioneering papers [1 – 19]. A.M. Prokhorov played a large role in the establishment of close cooperation between the scientists of the High Current Electronics Institute, Siberian Branch, Russian Academy of Sciences (HCEI SB RAS, Tomsk) and those of the General Physics Institute, Russian Academy of Sciences (GPI RAS, Moscow) in the development of pulsed gas lasers. Having commenced in 1973, this cooperation is being continued today [1 – 38].

Within the framework of this cooperation, investigations were made of CO_2 lasers pumped by an e-beam-controlled discharge [1, 2, 4, 7, 10, 11], an argon – nitrogen mixture laser pumped by an electron beam [3], and exciplex lasers utilising rare-gas halides [5, 6, 9, 11, 17]. A.M. Prokhorov lent impetus to research intended to model, with the aid of an electron beam, the conditions of nuclear pumping by pulsed reactors [18] as well as to research concerned with the investigations of gas discharges for lasers [13 – 17] and the interaction of laser radiation with matter [8, 12, 19]. High-power pulsed gas lasers nowadays enjoy wide use in different realms of science and technology (see books and reviews [39 – 55]).

Our review outlines the main results of the research on pulsed dense-gas lasers which were obtained in papers co-authored by A.M. Prokhorov and analyses their significance.

G.A. Mesyats Presidium of the Russian Academy of Sciences, Leninskii prosp. 14, 117901 Moscow, Russia;
V.F. Tarasenko High Current Electronics Institute, Siberian Branch, Russian Academy of Sciences, Akademicheskii prosp. 4, 634055 Tomsk, Russia; e-mail: VFT@loi.hcei.tsc.ru

Received 28 August 2002
Kvantovaya Elektronika **33** (7) 568 – 580 (2003)
Translated by E.N. Ragozin

2. Wide-aperture CO_2 lasers pumped by an e-beam-controlled discharge

The technique of high-pressure laser pumping with a discharge controlled or initiated by an electron beam enables designing wide-aperture lasers with a high output pulse energy. Initially, the electron beam injection into a gas was employed for the exact triggering of a high-voltage gap [56] and later for the production of a volume discharge in high-pressure CO_2 lasers [57, 58]. The first CO_2 laser [57] in which the electron beam was employed to stabilise the discharge could operate at a pressure up to 15 atm, while the first CO_2 amplifier [58] had an active volume of 1.5 L. We note that lasers pumped by a discharge initiated or controlled by an electron beam were, owing to their promise, vigorously investigated by numerous scientific groups both in the USSR and abroad. Even in 1973 there appeared reports on the development of lasers with an output pulse energy of 200 J [59] and 1000 J [60]. A short time later, laser systems were elaborated to deliver high-energy nanosecond pulses (180 J [61], 1 kJ [62], and 9 kJ [63]). In this Section we consider three wide-aperture CO_2 lasers and a high-pressure CO_2 laser, devised by staff members of the HCEI SB RAS and the GPI RAS, which yielded high output energies and exhibited a high efficiency. The elaboration of these lasers was made possible due to the development work financed in the HCEI SB RAS under the agreement with the GPI RAS.

2.1 Pulsed CO_2 laser with an output energy of 500 J [1]

The tests of this laser were completed in the GPI RAS late in 1974. For the first time it was possible to obtain the limiting efficiencies for pulsed atmospheric-pressure CO_2 lasers. The design of main laser units is shown in Fig. 1. These are an electron accelerator and a gas chamber with a resonator. The body (*1*) of the vacuum diode of the electron accelerator was made of stainless steel. The diode employed a multiple-pointed cold cathode (*2*) operating in the explosive emission mode [64, 65]. The working cathode area was 980×80 mm. The emitting 5-mm high apexes with

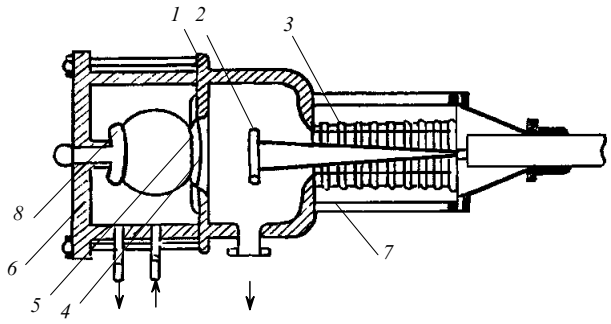

Figure 1. General view of the main units of the laser with an output energy of 500 J: (*1*) body of the vacuum diode; (*2*) multiple-pointed cold cathode; (*3*) insulator; (*4*) titanium foil; (*5*) grid; (*6*) gas cell; (*7*) metal cup; (*8*) anode.

a radius of curvature of 20 μm were uniformly distributed over the entire surface with a spacing of 4 mm. The departure of current density from the average value did not exceed 10 % throughout the beam cross section.

The electron beam was extracted through a window in the body of the vacuum diode measuring 1020×120 mm. The window was closed with a vacuum-tight titanium foil 50 μm in thickness. The cross sectional beam area was 1000×100 mm at exit from the foil, and the foil–cathode separation was equal to 80 mm. The diode employed a sectioned insulator (*3*) placed into a metal cup (*7*). The space between the inner cup wall and the insulator was filled with nitrogen at a pressure of 15 atm. The insulator presented its inner cavity to the vacuum diode, in which the pressure was equal to $\sim 10^{-4}$ Torr.

Provision was made to change the parameters of electron beam current (duration $t_b = 0.5 - 1.5$ μs, current density $j_b = 0.3 - 1.4$ A cm^{-2}). The pulse of electron beam current was nearly rectangular in shape. The average energy of the beam electrons remained invariable during the pulse and amounted to 200 keV, which ensured a uniform ionisation of the 10-cm deep gas volume at a pressure of 1 atm.

The body (*6*) of the gas cell was made of organic glass and was provided with end windows for the mounting and adjustment of the mirrors of the optical resonator. The employment of a dielectric gas cell allowed a significant simplification of laser design. An antiarc protective grid (*5*) was mounted near the foil. The anode (*8*) in the gas cell was shaped in such a way as to guard against a corona discharge.

The energy for the excitation of the active volume of the gas cell was stored in a bank of low-inductance capacitors with a capacity up to 8 μF. The capacitors were charged to 60 kV from a direct-current voltage source. The initial and residual (upon the completion of a discharge) voltages across the capacitor bank were recorded to enable a sufficiently accurate determination of the pump energy.

The knowledge of energy input into the active medium is of crucial importance in the analysis of CO_2-laser operation. The energy introduced into a unit volume of the gas medium is defined by the following relationship:

$$W_g = \frac{Cd^2E_0^2}{2V}\left\{1 - \exp\left[-2\left(\frac{\psi}{\beta}\right)^{1/2}\frac{\mu V e}{C}\frac{t_b}{d^2}\right]\right\}, \qquad (1)$$

where $\psi = j_b N_0 p \langle\sigma\rangle e^{-1}$; C is the capacitor bank capacitance; d is the spacing between the cathode and the anode; E_0 is the electric field intensity; $V = dS$ is the gas cell volume; β is the recombination coefficient; e is the electron charge; $\langle\sigma\rangle$ is the ionisation cross section; p is the gas pressure; and $N_0 = 2.7 \times 10^{19}$ cm^{-3} atm^{-1}.

The second term in braces specifies the fraction of energy that remains in the capacitor bank after completion of electron beam injection. This term is designated as K. A value $K = 0.5 - 0.7$ should be regarded as the optimal one. For larger K values, in the capacitor bank there remains a substantial amount of unused energy. For smaller K, the field intensity would become lower in the course of the pulse, resulting in impairment of the lasing conditions and efficiency lowering. In view of the aforesaid, from expression (1) we obtain the relationship

$$\frac{V\sqrt{\psi}}{Cd^2} = \frac{\ln(1/k)}{2t_b e\mu}\sqrt{\beta}, \qquad (2)$$

which proves to be quite useful in determining the relationship between the electron beam parameters, the gas properties, and the cell dimensions.

All experiments were conducted with a $CO_2 : N_2 : He = 1 : 1 : 3$ mixture, for which $\beta = 10^{-7}$ cm^3 s^{-1} V^{-1}. A plane-parallel KRS plate with a diameter of 150 mm and a single-surface reflectance of 17 % fulfilled the function of the output mirror of the laser resonator. A gold-coated quartz substrate served as the nontransmitting mirror. This enabled making a resonator with a large aperture and a high resistance to radiation damage. In operation, the optical elements of the resonator would withstand prolonged radiation loads up to 7.5 J cm^{-2} without damage. The radius of curvature of the nontransmitting mirror was equal to 5 m. The output radiation energy was measured by scanning across the laser-beam cross section an IKT-1M calorimeter whose detector head was devoid of a sapphire window. The results of the corresponding calculation were consistent with the data of check experiments performed with the use of radiation beam splitters, which were made on the basis of thin lavsan or polyethylene films. The radiation pulse shape was recorded with a Ge–Zn–Sb (77 K) photodetector with a time resolution of 1 ns. The FWHM duration of the output pulse was equal to 1 μs. The amplitude and shape of the output pulse remained practically invariable throughout the cross section of the laser beam, which is indicative of a high degree of excitation uniformity of the active laser medium.

Fig. 2 depicts the output energy and the efficiency of energy deposition as functions of field intensity. In the

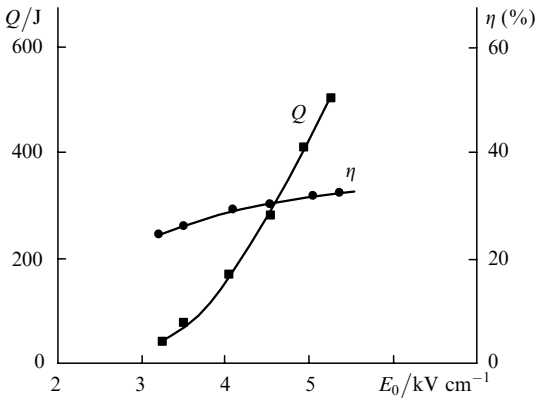

Figure 2. Output radiation energy Q and efficiency η as functions of field intensity.

$CO_2 : N_2 : He = 1 : 1 : 3$ mixture at atmospheric pressure, the highest radiant-energy extraction efficiency, calculated relative to the energy input, equal to 33 % is seen to occur for a ratio $E/p = 5.5$ kV cm^{-1} atm^{-1}. In this case, the energy input amounts to 150 J L^{-1} and the output energy to 500 J. We note that the highest CO_2-laser efficiency in Ref. [1] was overestimated by 15 % (in reality it was equal to about 28 %), as revealed by subsequent theoretical and experimental investigations.

2.2 Pulsed CO_2 laser with an output energy of 5 kJ [2]

The development of an atmospheric-pressure CO_2 laser with an active volume of 270 L ($30 \times 30 \times 300$ cm) was completed and its tests were conducted (also in the GPI RAS) in the mid-1975. The gas volume was ionised by an accelerated electron beam. The gas cell (*1*) (Fig. 3) with a volume of 4500 L was made of steel, and its inner surface was fettled with a glass-reinforced plastic (*3*) to guard against a corona discharge. The anode (*2*) of the gas cell with a working area of 30×300 cm was made of duralumin and was also shaped so as to guard against a corona discharge. The cell was filled a $CO_2 : N_2 : He = 1 : 1 : 3$ composition mixture to a pressure of 1 atm.

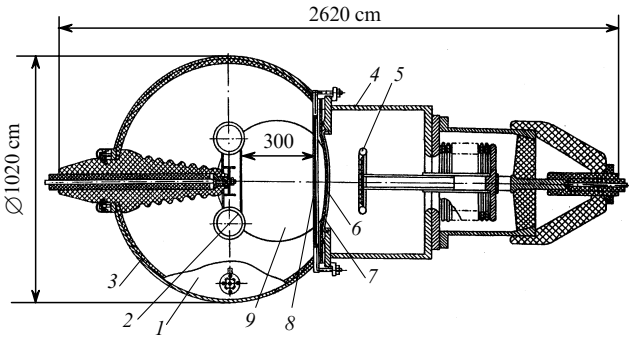

Figure 3. General view of the main units of the laser with an output energy of 5 kJ: (*1*) gas cell; (*2*) anode; (*3*) glass-reinforced plastic; (*4*) electron gun; (*5*) multiple-pointed cathode; (*6*) grid; (*7*) polymer film; (*8*) mesh; (*9*) nontransmitting mirror.

An electron gun (*4*) provided a uniform electron beam with a cross section of 30×300 cm. The average electron density was equal to 200 keV for a pulsed current density in the gas cell up to 0.4 A cm^{-2} and a duration of about 2 μs. The vacuum diode employed a multiple-pointed cold cathode (*5*) operating in the 'explosive emission' mode. The beam was extracted from the vacuum diode of the electron gun through a window covered with a 150-μm thick polymeric film (*7*) supported by a metal grid (*6*). Upon evacuation of the diode, the film deflection did not exceed 18 mm. The discharge current in the gas laser cell was closed at a steel mesh (*8*), which protected the film from the thermal action of the discharge. The net transmittance of the window and the mesh for electrons with energy of 200 keV was no less than 50 %. The diode of the electron gun was fed from a Marx pulse voltage generator with a shock capacitance of 0.67 μF and an output voltage of 500 kV. The energy that went to excite the active volume of the gas cell was stored in a capacitor bank assembled of low-inductance capacitors. The maximum parameters of the capacitor bank: a capacitance of 15 μF, a charging voltage of 200 keV, and a stored energy of 300 kJ.

Fig. 4 shows the measurement data for the pump energy inputted into the gas laser volume. The laser operation was stable when the voltage applied to the anode in the gas cell did not exceed 125 kV (i.e., when the field intensity in the gas did not exceed 4.2 kV cm^{-1}). In this case, the highest amplitude of gas discharge current was equal to 150 kA for a FWHM pulse duration of 2 μs. The laser employed a resonator with an output mirror with diameter of 240 mm made of a plane-parallel KRS8 plate with a single-surface reflectance of 17 %. A gold-coated quartz substrate (*9*) with a radius of curvature of 12 m and diameter of 300 mm fulfilled the function of the nontransmitting mirror. The mirrors employed did not allow extracting energy from the entire volume under excitation. Nevertheless, the total output energy in the optimal operating conditions measured by scanning the calorimeter across the lateral section of the laser beam amounted to 5 kJ.

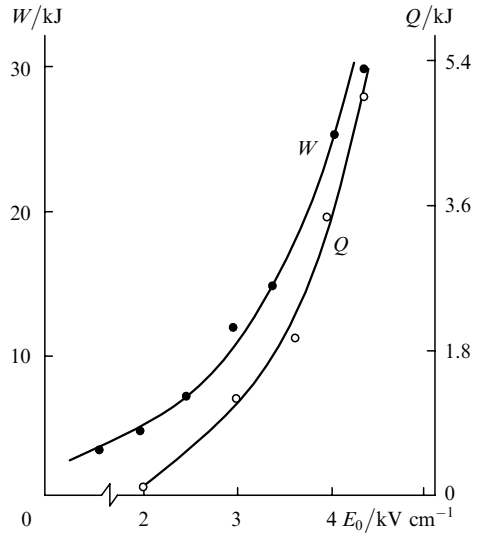

Figure 4. Pump energy W and output radiation energy Q as functions of field intensity.

Fig. 4 also shows the dependence of output laser energy on the electric field intensity in the gas. The peak radiation energy density amounted to 20 J cm^{-2} in the central region of the beam and to 9 J cm^{-2} at the periphery of the beam. The FWHM duration of the output pulse was 1.5 μs. Such a high radiation energy density resulted in the emergence of defects in the material of the output resonator mirror upon prolonged operation. Since the active volume of the gas cell exceeded the gas volume in the resonator by about a factor of two, there existed a possibility to increase the output energy by increasing the dimensions of the optical elements. This was accomplished in Ref. [4], in which the output pulse energy amounted to 7.5 kJ upon optimisation of the resonator. Note that this laser at one time was among the world's highest output-energy lasers.

2.3 Matched-mode excited CO_2 laser with an output energy of 3 kJ [10]

This laser, which is depicted in Fig. 5, was put into operation and investigated in the HCEI SB RAS. The facility consisted of a gas chamber, a power supply, and an electron accelerator. The active medium was excited by a nonself-sustained discharge. The maximum volume of the chamber

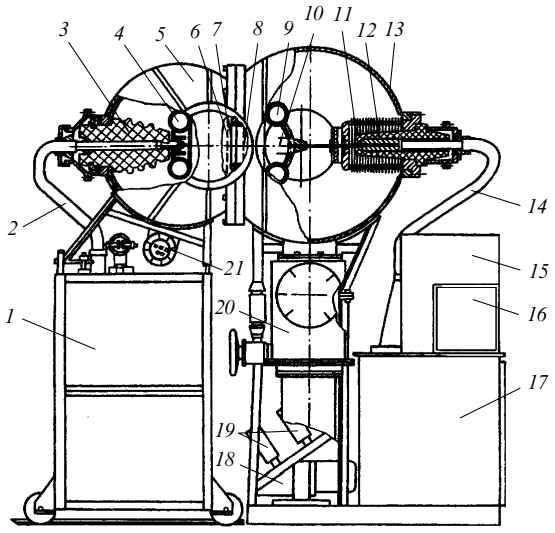

Figure 5. Laser design: (*1*) PVGs that feed the laser gap; (*2*), (*14*) KPV-7-300 cable; (*3*), (*12*) insulators; (*4*) anode; (*5*) body of the laser chamber fettled with a dielectric; (*6*) mesh; (*7*) foil or lavsan film; (*8*) extractor; (*9*) cathode screen; (*10*) emitters; (*11*) sectional insulator; (*13*) body of the vacuum diode; (*15*) control desk; (*16*) triggering unit; (*17*) accelerator PVG; (*18*) pump; (*19*) electromagnetic valves; (*20*) vacuum pump unit; (*21*) gap.

with the active medium was 50 L ($20 \times 20 \times 125$ cm). The laser chamber allowed operating at a pressure as high as 2.5 atm. It was originally conceived that this laser would be employed as a short-pulse amplifier, and the laser was therefore intended for operation at high pressures and high specific pump powers to increase the gain coefficient. Experiments were carried out with an active volume of 50 L as well as with a reduced active volume (12 L, $8 \times 12 \times 125$ cm). The electron accelerator provided an electron beam with a current density in the gas chamber of the order of 0.5 A cm^{-2} for an accelerating voltage in the vacuum diode of ~ 300 kV.

The oscilloscope traces of accelerating voltage across the vacuum diode and the electron beam current in the gas chamber are shown in Fig. 6a and 6b. A specific feature of the selected laser operating mode was that the pulse of the electron beam was twice as long as the discharge current pulse. The discharge in the chamber was delayed relative to the beam by approximately 0.3 μs (Fig. 6c). Therefore, the pumping was effected at about constant values of the beam current density and electron energy. This was of significance in maximising the specific pump and output energies. We took advantage of an *LC* correction in the pulse voltage generator (PVG) which fed the vacuum diode, which enabled us to obtain a nearly rectangular-shaped beam current pulse (Fig. 6b).

To feed the gas chamber, use was made of a Marx PVG consisting of three parallel branches with five stages in each of them. The PVG employed IK-100/0.4 capacitors and the *LC*-correction circuit employed IMN-100/0.1 capacitors. The equivalent PVG capacitance was 0.24 μF and the wave impedance was $\rho = 3.3\ \Omega$; for a charging voltage $U = 58$ kV, the energy stored in the PVG was equal to 10 kJ. The PVG employed gaps blown out with dry air to ensure a high actuation stability (±20 ns), which allowed timing the discharge current pulses in the gas chamber with the beam current pulses. To find out whether high energy

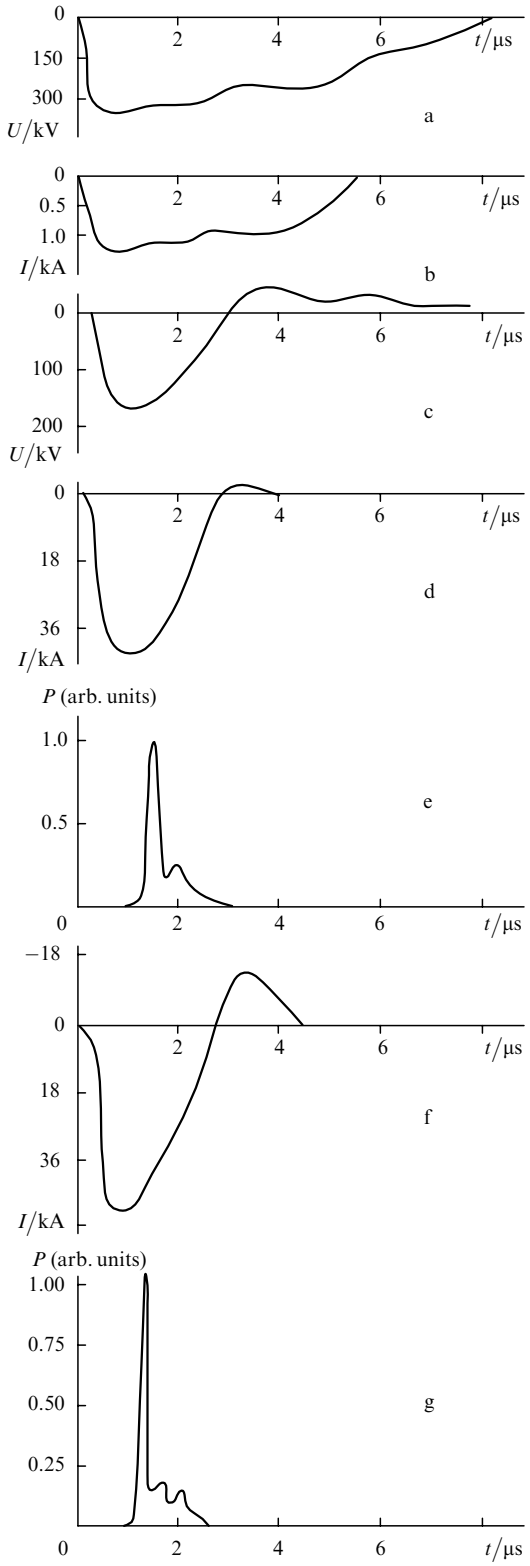

Figure 6. Oscilloscope traces of accelerator voltage (a) and current (b) pulses, voltage pulses across the laser gap (c), pulses of current through the laser chamber (d, f), and output radiation pulses (e, g) for a $CO_2 : N_2 : He = 1 : 2 : 2$ mixture at a pressure $p = 2$ atm and an active medium volume of 50 (c–e) and 12 L (f, g); the charging PVG voltage is 58 kV.

inputs can be realised in the matched mode, the volume of the active medium was reduced to 12 L ($8 \times 12 \times 125$ cm). The limited energy store of the PVGs feeding the discharge

gap did not permit doing this for a volume of 50 L. When the active volume was reduced to 12 L, the plasma resistance lowered to 2.5 Ω. The internal resonator was made up of a copper mirror and a plane-parallel plate of KRS5 or NaCl accommodated at the ends of the laser chamber.

In the laser with an active volume of 50 L, for a $CO_2:N_2:He = 1:2:2$ mixture at a pressure of 2 atm the plasma resistance was equal to 3.8 Ω. Fig. 6 shows the oscilloscope traces of the pulses of voltage across the plasma and discharge current as well as of output pulses. The dependence of total output energy on the energy stored in the PVG is depicted in Fig. 7a. The output energy was nonuniformly distributed over the lateral section of the output beam; the energy density at the centre was as high as 15 J cm^{-2}, and damage of the output window was observed in this case. The maximum total output energy was equal to 3 kJ and the efficiency to ~ 25 %. The oscilloscope traces of discharge current and output pulse pertaining to this case are shown in Figs 6d and 6e. The fraction of energy inputted into the gas during the second half-cycle of current did not exceed 10 %, and therefore the mode can be treated as a matched one.

Fig. 7b shows the dependences of specific output energy on the energy input at mixture pressures of 2 and 1.2 atm as well as for different resonators wherein the function of output mirrors was fulfilled by NaCl and KRS plates. The maximum output energy extracted from the 12-L volume was equal to 1.8 kJ. The amplitude value of voltage across the plasma was 136 kV ($E/p = 8.5$ kV cm^{-1} atm^{-1}), and the highest energy inputs were in excess of 0.6 kJ L^{-1} atm^{-1}. The paper under review reported for the first time the attainment of maximum energy extraction from a unit volume of the active medium equal to 150 J L^{-1}. We note that the efficiency of lasing lowered with increase in specific energy input.

Therefore, the employment of an e-beam-controlled discharge for pumping wide-aperture CO_2 lasers ($\lambda =$ 1.06 μm) permits obtaining high output energies and high efficiencies at high pressures. Atmospheric-pressure lasers with active volumes of 10 and 270 L yielded output energies of 0.5 and 7.5 kJ, respectively; a laser with a 50-L volume of the active medium for a working mixture pressure of 2 atm and a pulse feeding of the laser gap delivered an output energy of 3 kJ. The highest output efficiency of lasers of this type amounted to ~ 28 %. With a pulsed feeding of the discharge gap it was possible to obtain specific pump and output energies of 0.6 kJ L^{-1} atm^{-1} and 80 J L^{-1} atm^{-1}, respectively.

In 1986, the pumping system of the CO_2 laser with an active volume of 270 L was employed to investigate lasing in the near-IR spectral region on atomic xenon transitions [27]. Owing to the large interelectrode gap it was possible to obtain lasing under pumping by a nonself-sustained discharge (both with and without ionisation multiplication) and demonstrate that the electric field makes a contribution to the output energy only with ionisation multiplication of electrons.

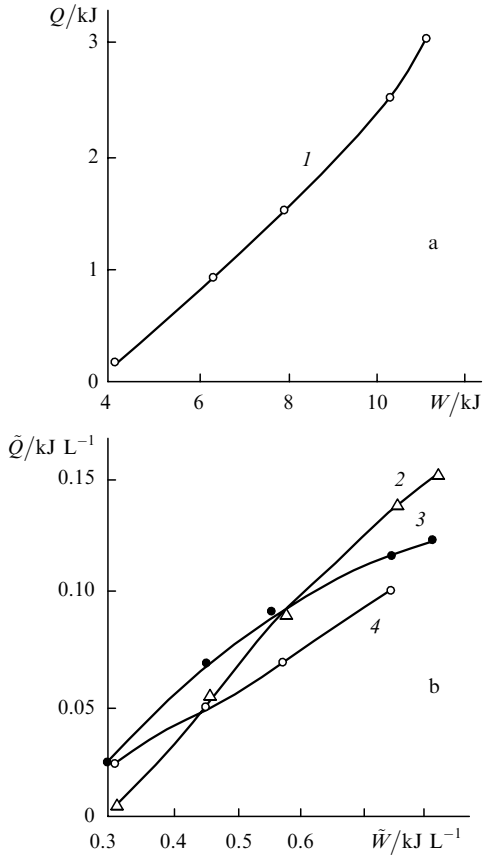

Figure 7. Dependences of the total output energy on the energy input for an active medium volume of 50 L (a) and of specific output energy on specific energy input for an active medium volume of 12 L (b). A $CO_2:N_2:He = 1:2:2$ mixture at pressures $p = 2$ (*1–3*) and 1.2 atm (*4*); the output mirror is made of KRS5 (*1*, *3*, *4*) and NaCl (*2*).

2.4 Continuously frequency-tunable high-pressure CO_2 laser [7]

The production of short high-power radiation pulses and the expansion of frequency tuning range involve increasing the pressure and volume of the active medium under excitation with retention of a high gain coefficient. This problem is solved with the use of an e-beam controlled nonself-sustained discharge as the pump. The facility is diagrammed in Fig. 8. The active medium was ionised by 1-μs long electron beam with a density of 2 A cm^{-2} and a cross section of 3×100 cm. The anode–cathode separation in the gas chamber could be varied between 1 and 3 cm. The energy expended on the excitation of the active medium was stored in a low-inductance capacitor bank (*2*) with a capacitance of 0.8 μF. This laser is described in greater detail elsewhere [66].

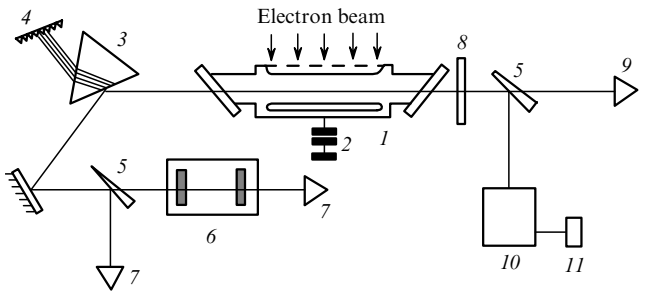

Figure 8. Schematic of the tunable CO_2 laser: (*1*) CO_2 laser module; (*2*) capacitor bank (0.8 μF, 100 kV); (*3*) NaCl prism; (*4*) diffraction grating; (*5*) ZnSe plates; (*6*) interferometer; (*7*) IMO-2 calorimeter; (*8*) output mirror; (*9*) IKT-1M calorimeter; (*10*) monochromator; (*11*) pyroelectric detector.

The dispersion resonator was formed by a 150-lines mm^{-1} diffraction grating (*4*), a plane-parallel germanium plate with one antireflection-coated face, and a NaCl prism (*3*), which provided an eight-fold increase in the beam aperture at the grating. The resonator aperture was limited by two aperture stops 6 mm in diameter to ensure a single-mode laser operation. The grating was mounted accurate to 10″.

To measure the spectral characteristics, use was made of a monochromator (*10*) with a resolution of 0.3 cm^{-1} and a scanning Fabry–Perot interferometer (*6*) with a base length of 2.5 cm and a finess of 30, which allowed measuring the tuning characteristics and the laser line width.

A nonself-sustained discharge effected the excitation, the bulk of energy being inputted in the fields with intensities of 4–11 kV cm^{-1} atm^{-1}. A $CO_2:N_2 = 1:1$ mixture proved to be optimal under these conditions. The limiting energy dissipated in the gas at a mixture pressure between 4 and 6 atm was equal to 250–300 J L^{-1} atm^{-1}. The limiting lasing energy that did not result in the failure of optical elements was equal to 1–1.5 J cm^{-2} and was reached throughout the range of continuous frequency tuning. The FWHM duration of the output pulse did not exceed 40 ns. The tuning characteristics of the laser, i.e., the dependences of laser frequency on the grating rotation angle, were investigated throughout the possible CO_2-laser oscillation range.

Continuous frequency tuning became possible even at a pressure of 4 atm. However, a significant nonlinearity of the tuning characteristic due to the laser frequency pulling to amplification line centres was a hindrance to the practical use of this regime. Raising the mixture pressure to 5 atm made the tuning characteristics practically linear. The spectral width of the laser line measured with the aid of a scanning interferometer with a base length of 2.5 cm was equal to 0.028 cm^{-1} for the *P*18 line and to 0.24 cm^{-1} in the dip between the *P*16 and *P*18 lines of the 001–100 transition. The resonator with a germanium output mirror ensured a continuous tuning range of 86 cm^{-1} at a pressure of 6 atm (the *P*6–*P*34 and *R*6–*R*30 lines of the 001–100 and 001–020 transitions).

Further broadening of continuous tuning range is possible through the increase in gain of the active laser medium, which involves increasing the specific pump energy. However, increasing the energy introduced into the gas may result in the occurrence of superfluorescence, making the laser uncontrollable in frequency. This leads to the limitation of energy inputs when the laser is operated in the mode of radiation frequency tuning. Fig. 9 shows the specific energy input whereby the superfluorescence threshold is reached as a function of mixture pressure. Curve (*2*) corresponds to the threshold of lasing in the dip between the *P*16 and *P*18 lines. The domains bounded by curves (*1*) and (*2*), as well as (*1*) and (*3*), define the energy inputs required for laser operation in the mode of continuous frequency tuning.

Therefore, the employment of an e-beam-controlled nonself-sustained discharge made it possible to devise a high-pressure CO_2 laser continuously tunable over a 86-cm^{-1} band for an output radiation energy density of 1.5 J cm^{-2} (the maximum radiation energy density for a fast damage of the optics is no greater than 5 J cm^{-2}). This laser was employed for many tasks, and in particular for the selective excitation of gases in the strong IR laser field [8].

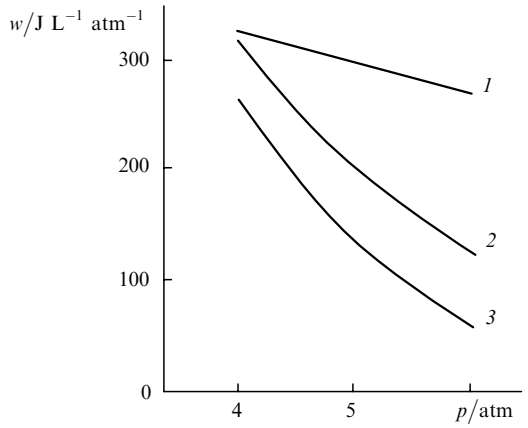

Figure 9. Value of specific energy input at which the lasing threshold is reached as a function of mixture pressure [(*1*) superfluorescence threshold, (*2*) threshold of lasing at the dip between the *P*16 and *P*18 lines, (*3*) threshold of lasing on the *P*18 line].

3. Investigation of oscillation in an Ar–N_2 mixture laser [3]

In the 1970s, a start was made on intensive studies of lasers pumped by an electron beam. Unlike xenon dimer lasers, an Ar–N_2 mixture laser had a low lasing threshold, was operated at relatively low pressures of the working mixture, which consisted of inactive gases, and enabled obtaining radiation in the UV and visible spectral regions. This laser was comprehensively investigated in the HCEI SB RAS, and the publication of the first results was supported by A.M. Prokhorov [3]. The laser utilises mixtures containing nitrogen and argon. The electron beam energy goes primarily into the ionisation and excitation of argon and then, owing to the effective energy transfer from metastable (3*p*) argon levels to the $C^3\pi_u$ level of the nitrogen molecule, there emerges inversion on the $C^3\pi_u \rightarrow B^3\pi_g$ transition. Lasing was obtained on the transitions 0–0 ($\lambda = 337$ nm), 0–1 ($\lambda = 358$ nm), 0–2 ($\lambda = 381$ nm), etc. Owing to the retention of optimal pump conditions (the electron temperature) during the action of the electron beam and to the participation of argon in the depopulation of the lower laser level, the Ar–N_2 mixture laser enables realising long output pulse durations (hundreds of nanoseconds – few microseconds).

To excite the Ar–N_2 mixture in Ref. [3], use was made of a ribbon-shaped electron beam with the following parameters: an electron energy of 400 keV, a beam current density of 200 A cm^{-2}, the FWHM duration of the beam current of 13 ns, and a lateral beam section measuring 20×1 cm. The electron accelerator could operate with the laser chamber in a single-pulse mode and in the mode of two pulses with a controllable delay between them. Without the laser chamber and with blowing on the foil, the accelerator had the capacity for short-term service with a repetition rate up to 150 Hz.

The laser chamber was made in the form of a tube 2 cm in diameter. The electron beam was injected into the gas volume through a 50-μm thick steel foil transversely to the optical axis. The total electron current that reached the laser chamber amounted to 4.3 kA. The resonator was formed by a plane aluminium-coated mirror and a plane-parallel quartz plate.

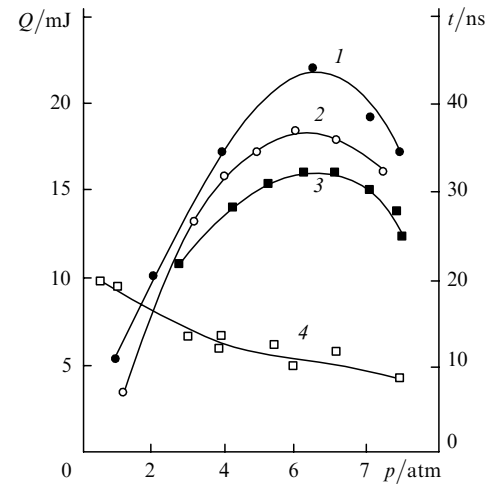

Figure 10. Output energy (*1–3*) and the FWHM duration of the laser pulse (*4*) as functions of the total $Ar-N_2$ mixture pressure for a nitrogen density of 10 % (*1*, *4*), 14 % (*2*), and 5 % (*3*).

Fig. 10 shows the energy and the FWHM duration of the laser pulse versus mixture pressure for different nitrogen densities. The output energy peaked at pressures of 6–8 atm. The dependences of output energy and FWHM duration of the laser pulse on the percentage of nitrogen in the mixture are given in Fig. 11, in this case the working pressure for each point of the curve corresponding to the maximum output energy. Increasing the resonator quality factor results in a decrease of the output laser energy. With the use of only the nontransmitting mirror (the output mirror was misaligned), the laser could operate in the superfluorescence mode, but the output energy was several times lower.

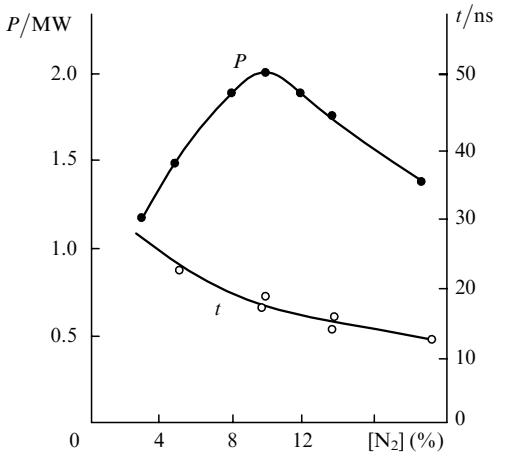

Figure 11. Output power and the FWHM duration of the laser pulse as functions of nitrogen content in the mixture.

For low pressures and low nitrogen densities, the FWHM duration of the output laser pulse exceeds the duration of the pump pulse. For the maximum laser energy and power equal to 22 mJ and 2 MW, the FWHM duration of the output pulse corresponded to about half the pump pulse duration. In this case, the pressure of the $Ar:N_2 = 9:1$ mixture was equal to 6.5 atm. The lasing efficiency of the $Ar-N_2$ mixture laser is low in comparison with the efficiency of rare-gas halide exciplex lasers, and in the experiments of Ref. [3] it did not exceed 0.3 %, if the calculation of energy inputted into gas is made more exact by taking into account the nonlinearity of the trajectory of the beam electrons and the electron reflection from the walls of the laser chamber.

A method of excitation by double current pulses injected into the laser chamber with a controllable delay makes it possible to elucidate the potentialities of laser operation in the pulse-periodic regime. Fig. 12 depicts the ratio between the laser power in the second pulse and the laser power in the first pulse as a function of repetition frequency of the two pulses. One can see that the laser pulses are equal in power up to 20 Hz. At a frequency of 50 Hz, the power of the second pulse is lower by 40 %. Ref. [3] marked the beginning of a series of investigations pursued by the staff members of the HCEI SB RAS to study the $Ar-N_2$ mixture laser [25, 67–70], which yielded the following results:

– For the first time it was possible to realise high-power lasing simultaneously at three lines $\lambda = 337$, 358, and 381 nm in an $Ar-N_2$ mixture and demonstrate the feasibility of discrete tuning of the radiation wavelength.

– Additions of helium and neon were shown to increase the power of spontaneous radiation at the second positive system of nitrogen and the efficiency of lasing in an $Ar-N_2$ mixture pumped by an electron beam.

– The effect of the pump power on the duration of inversion maintenance in lasers utilising self-terminating transitions was analysed, and increasing 'useful' pump duration was shown to increase the duration of the laser pulse.

– An output radiation energy of 3 J, a specific output energy up to 0.12 J l-1, and the FWHM duration of the radiation pulse of 290 ns were obtained on a facility with an active volume of 30 L in an $Ar-N_2$ mixture.

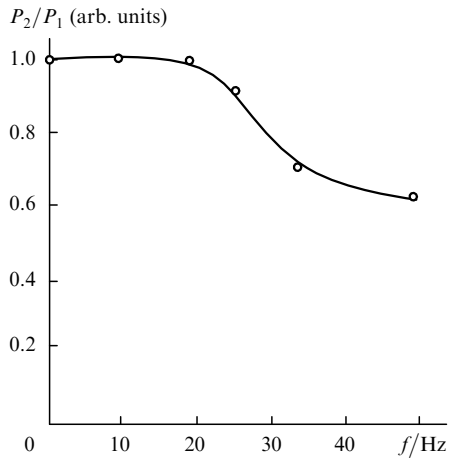

Figure 12. Second-to-first pulse power ratio as a function of pulse repetition rate.

4. Exciplex lasers utilising rare-gas halides (first experiments)

The research aimed at the development of exciplex lasers pumped by an e-beam initiated discharge and pumped by an electron beam was undertaken by staff members of the HCEI SB RAS in 1977 [5, 71]. At that time, the pioneering papers on the first rare-gas halide lasers put into operation

in the USA were already well known (see Refs [72–74] and also references in the books and reviews [41, 42, 44, 46–48, 50, 52]). Refs [5, 6, 9, 11, 12, 17, 19], which were backed up by A.M. Prokhorov, reported the research on different exciplex lasers and their applications.

4.1 Exciplex laser utilising XeF^* molecules ($\lambda \sim 350$ nm) pumped by a discharge controlled by a microsecond electron beam

The experiments of Ref. [6] were conducted employing the pump system of the high-pressure CO_2 laser described in detail in Ref. [66]. The facility comprised an electron accelerator, which produced an electron beam with a duration of 1 μs, a current density above 2 A cm^{-2}, and an electron energy of ~ 200 keV, and a laser chamber with an active volume measuring $1.8 \times 3 \times 100$ cm. The electron beam was injected into the discharge gap through a window covered with a 50-μm titanium foil. The discharge was fed from a storage capacitor connected to the electrodes of the discharge chamber via a current shunt. The working mixtures consisted of argon, xenon, and SF_6; the maximum mixture pressure was equal to 5 atm.

Fig. 13 shows the dependence of output energy on the mixture pressure for different charging voltages and mixture compositions. The highest-energy laser pulse (0.2 J) was produced at a pressure of 5 atm and a charging voltage of 23 kV, in this case the efficiency was equal to ~ 0.3 %. The output power was significantly lower when the pumping was effected by the electron beam alone. It is pertinent to note that, along with UV lasing by XeF^* molecules ($\lambda \sim 350$ nm), observations were made of IR lasing on atomic xenon transitions under these conditions. At a pressure of 5 atm and a charging voltage of 23 kV, the fraction of the IR lasing was within 20 % of the UV lasing. However, on reducing the specific energy input by lowering the charging voltage and (or) the capacitance of the storage capacitor, and also under pumping by the electron beam alone, the fraction of IR radiation could be as high as 90 %. We also note that the IR-to-UV lasing ratio is significantly affected by the resonator employed. Simultaneous lasing in the UV and IR spectral ranges was investigated comprehensively in Ref. [75] for a XeCl laser pumped by a microsecond electron beam.

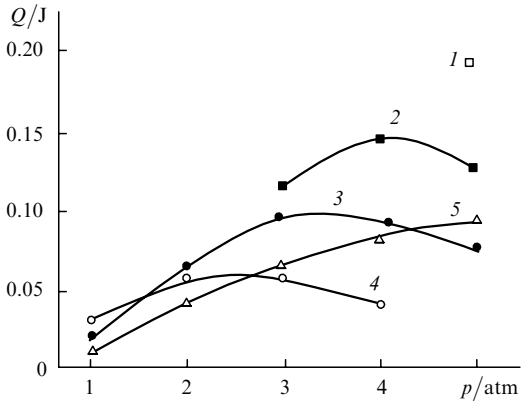

Figure 13. Output energy as a function of mixture pressure for a charging voltage of 23 (*1*), 14 (*2*), and 10 kV (*3–5*) for $Ar:Xe:SF_6 = 2200:10:1$ (*1–3*), $Ar:Xe:SF_6 = 1000:10:1$ (*4*), and $Ar:Xe:SF_6 = 3500:10:1$ (*5*) mixtures.

4.2 Exciplex laser utilising $XeCl^*$ molecules ($\lambda \sim 308$ nm) pumped by a discharge initiated by a nanosecond electron beam [6]

The experiments employed a facility comprising a 300-keV electron energy accelerator, a beam current density of 40 A cm^{-2}, and the FWHM duration of the beam current as well as a discharge chamber with an electrode separation of 2 cm. The electron beam was injected into the discharge gap through a window covered with a 25-μm iron foil. The discharge was fed from a low-inductance capacitor bank assembled of K15-4 capacitors (2200 pF, 30 kV), which was connected to the electrodes of the laser chamber via a current shunt. The resonator was made up of an aluminium-coated plane nontransmitting mirror and a plane-parallel quartz plate. The working mixtures contained Ar, Xe, and CCl_4, which were prepared in a mixer prior to admission to the laser chamber.

Fig. 14 shows the dependence of output pulse energy on the mixture pressure and the capacitance of the storage capacitor, and Fig. 15 depicts the oscilloscope traces of output pulses and discharge current. The output laser energy increased with charging voltage up to the static breakdown voltage. The discharge became oscillatory at voltages close to the static breakdown one (Fig. 15d). The highest efficiency of lasing was reached for an aperiodic discharge and a charging voltage that was ~ 25 % lower than the static breakdown voltage for the gap involved. With the use of a combined pumping (by the electron beam

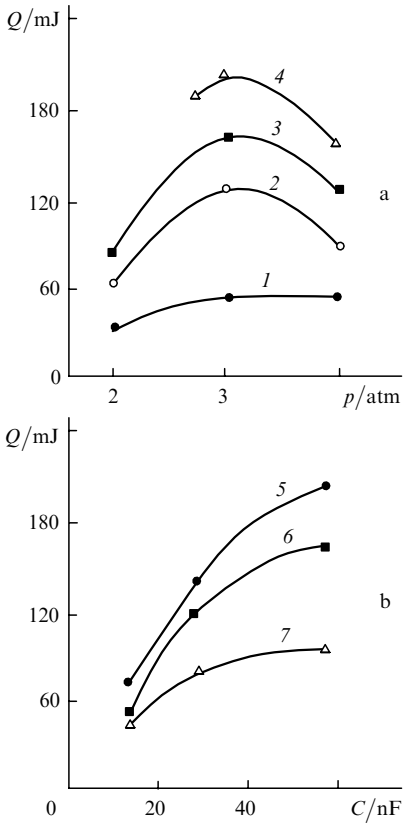

Figure 14. Output laser energy as a function of mixture pressure (a) and capacitance of the storage capacitor (b) (an $Ar:Xe:CCl_4 = 1600:50:1$ mixture) under pumping by an electron beam (*1*) and an e-beam initiated discharge for a charging voltage of 12 (*2*), 16 (*3*), and 20 kV (*4*) ($C = 57$ nF) as well as for $U_0 = 20$ kV, $p = 3$ (*5*) and 4 atm (*6*); $U_0 = 16$ kV, $p = 2$ atm (*7*).

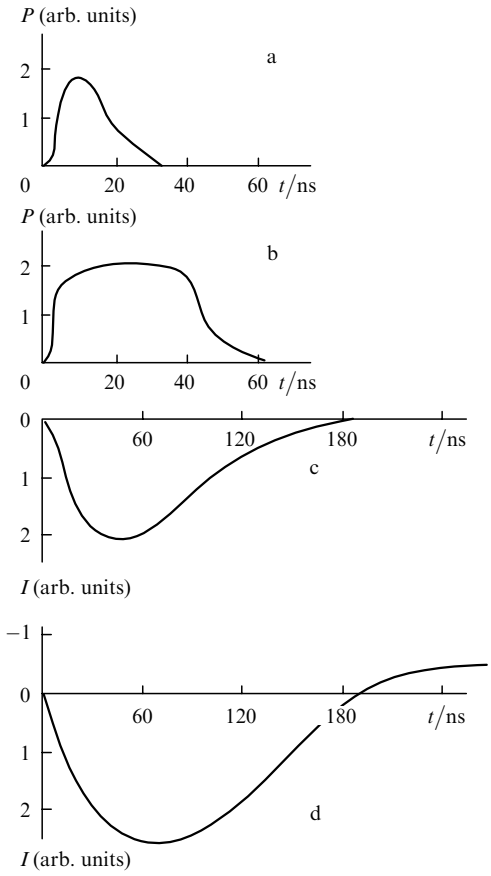

Figure 15. Oscilloscope traces of laser pulses (a, b) and current (c, d) under pumping by an electric beam alone (a) and by an e-beam initiated discharge for $U_0 = 20$ kV, $C = 57$ (b, d) and $C = 28.5$ nF (c); the $Ar : Xe : CCl_4 = 1600 : 50 : 1$ mixture pressure is equal to 3 atm.

and the discharge) the output energy was more uniformly distributed over the lateral section of the output beam.

Therefore, in Ref. [6] for the first time it was possible to obtain a high efficiency of lasing (2 %) by $XeCl^*$ molecules ($\lambda \sim 308$ nm) excited by the electric field of a capacitive storage device with e-beam initiated discharge pumping.

4.3 Lasing by XeF^* ($\lambda \sim 350$ nm), $XeBr^*$ ($\lambda \sim 282$ nm), and $XeCl^*$ ($\lambda \sim 308$ nm) molecules pumped by an e-beam-controlled discharge [9, 11]

The experiments employed the CO_2-laser pump system shown in Fig. 5 and described in detail in Section 2.3, which was somewhat modernised. The facility comprised an electron accelerator, which produced an electron beam with a duration of 1 or 5.4 μs, a current density up to 8 A cm^{-2}, and an electron energy of ~ 250 keV, and a laser chamber with an active volume measuring $20 \times 10 \times 140$ cm or $10 \times 5 \times 140$ cm, where the electrode separation was equal to 10 and 5 cm, respectively. A storage capacitor ($C = 3$ nF) was connected to the anode, the inductance of the discharge current was equal to 150 nH. In the investigations of lasing by rare-gas halide molecules, the mixture pressure was equal to 2 atm, the volume of the active medium of XeF and XeBr lasers was equal to 28 L and of a XeCl laser to 7 L. The working mixtures comprised argon, xenon, and one of the halogen-bearers (NF_3, $C_2F_4Br_2$, or CCl_4).

The highest output energy (25 J) was obtained with XeF^* molecules for an active medium volume of 28 L and a discharge pumping with ionisation multiplication. Fig. 16 shows the dependences of specific laser energy and energy inputted into gas on the charging voltage. One can see that the imposition of electric field leads to a significant increase in laser energy. Realised for highest laser energies is the regime of a volume discharge with ionisation multiplication, with discharge contraction upon cessation of the beam current. With $XeBr^*$ molecules, the laser energy did not exceed 9 J for the same active volume. The lowest laser energy equal to 3 J was obtained with $XeCl^*$ molecules. In the last-mentioned case, the volume of the active medium was reduced to 7 L. As already noted, the radiation of exciplex lasers utilising mixtures of a buffer argon gas and the principal xenon gas contains, along with UV laser radiation of exciplex molecules, the IR radiation arising from the transitions of atomic xenon. The fraction of this energy depends on the pump power, the mixture composition and pressure, and also the type of resonator in use. Under optimal conditions of exciplex laser operation, the fraction of IR radiation is smaller than 10 %. However, the IR radiation of xenon can make the main contribution to lasing for lower pump powers.

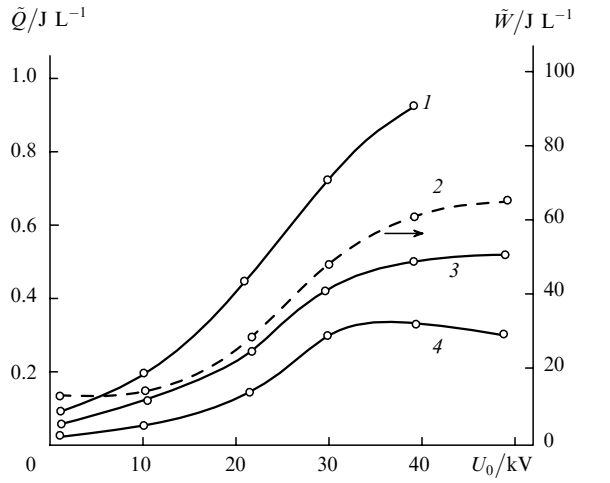

Figure 16. Specific laser energy $\tilde{Q}$ (*1*, *3*, *4*) and specific energy inputted into gas $\tilde{W}$ (*2*) as functions of charging voltage: an $Ar : Xe : NF_3 = 1000 : 10 : 1$ mixture, a beam current density $j = 3$ A cm^{-2}, and the FWHM pulse duration $\tau = 1.2$ μs (*1*), an $Ar : Xe : NF_3 = 2000 : 10 : 1$ mixture, $j = 1.2$ A cm^{-2}, and $\tau = 1$ μs (*2*, *4*), an $Ar : Xe : NF_3 = 2000 : 10 : 1$ mixture, $j = 3$ A cm^{-2}, and $\tau = 1.2$ μs (*3*).

The above experiments were conducted on a wide-aperture laser and allowed gaining the first experience of high-power exciplex laser development. An energy of 25 J per pulse at that time was highest for exciplex lasers elaborated in the USSR. The accumulated data showed that pumping with an electron beam alone is more expedient when we are to devise exciplex lasers with an output energy above 100 J. This was realised in more recent works performed in the HCEI SB RAS [52, 76, 77], which was the site of development of a XeCl laser with an output energy of ~ 2 kJ and a KrF laser with an output energy of ~ 100 J.

4.4 XeCl laser pumped by an X-ray preionised discharge [17]

At the present time, X-rays are extensively used in exciplex laser preionisation systems. The design of our first laser in which a volume discharge was initiated by X-rays is diagrammed in Fig. 17 [17]. This is a modification of the facility with pumping by an e-beam-controlled discharge; a similar facility was employed in Ref. [6] (see also Section 4.2) for the excitation of a XeCl laser. X-rays were produced due to the deceleration of a fast-electron beam in a tantalum foil (*2*) in a vacuum diode (*1*). The vacuum gap with a ribbon-shaped cathode was fed from a pulse-forming line (*5*) filled with glycerine. The current pulse duration was equal to 40 ns for a voltage of ~ 200 kV. The line (*5*) was charged from an Arkad'ev–Marx PVG. The laser gap was formed by a profiled electrode (*4*) and a plane electrode (*3*) made of a fine mesh or a copper foil. The electrode spacing was equal to 2.7 cm and the active length to 48 cm. The resonator was formed by an aluminium-coated mirror and a plane-parallel quartz plate. The $Ar:Xe:CCl_4 = 1000:10:1$ working mixture was prepared in the laser chamber. The investigations were carried out at pressures up to 3 atm. The pumping was effected from capacitors C_0 and C, the peaking capacitors C being evenly distributed along the length of the laser chamber. The voltage application to the electrodes in the laser chamber was timed with the X-ray burst by adjusting the triggering of a gap (*6*).

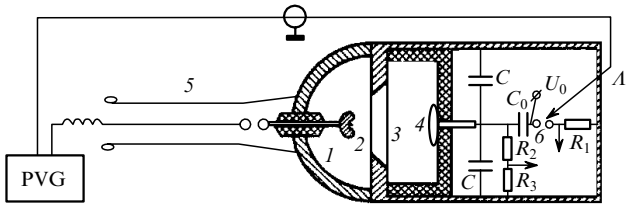

Figure 17. Laser design: (*1*) vacuum diode; (*2*) tantalum foil; (*3*) electrode; (*4*) profiled electrode; (*5*) charging line; (*6*) gap.

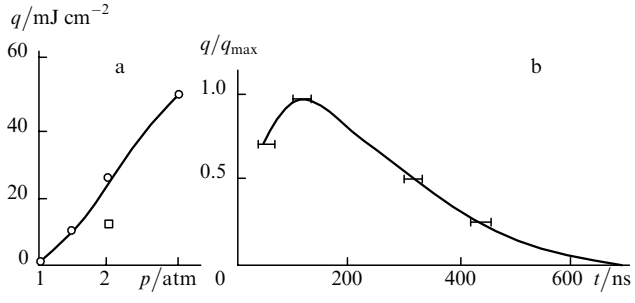

Figure 18. Dependences of the output energy density on the mixture pressure (a) and the delay between the onset of current buildup and the voltage across the laser gap for $p = 2$ atm (b) for the $Ne:Xe:CCl_4 = 1000:50:1$ mixture with $U_0 = 24$ kV; the plane electrode was made of a copper foil (○) or a mesh (□).

The experiments conducted revealed that the laser energy increases with mixture pressure and the optimal delay between the onset of the X-ray burst and the voltage application to the electrodes in the laser chamber is equal to 100–200 ns (Fig. 18). The state of electrode surface is of major importance. The highest specific output energy (above 1 J L^{-1}) was obtained when the mesh electrode was replaced with a foil electrode at the highest pressure possible in these experiments (3 atm). Measurements of the initial electron density showed that it amounts to $\sim 4 \times 10^{11}$ cm^{-3}.

The utility of lowering the X-ray photon energy to ~ 50 kV was also shown in Refs [16, 17]. This X-ray photon energy is already high enough for the preionisation in wide-aperture electric discharge lasers.

Therefore, the first papers concerned with exciplex laser research yielded the following results. A laser utilising XeF^* molecules pumped with a discharge controlled by a microsecond electron beam was put into operation. For the first time it was possible to obtain a high efficiency from the electric field of a capacitive storage device (2 %) of a XeCl laser pumped by an e-beam initiated discharge. When the volume of the active medium was increased to 28 L, the laser utilising XeF^* molecules pumped by an e-beam controlled discharge yielded an output energy of 25 J. More recently, investigations were made of XeF ($\lambda = 350$ nm), XeCl ($\lambda = 308$ nm), and XeBr ($\lambda = 282$ nm) lasers pumped by electron beams of different duration as well as by e-beam-controlled discharges, and the inversion production mechanisms were shown to be essentially different in these lasers [50, 52].

5. Determination of NO_2 and CO admixtures in the atmosphere [19, 78]

Modern advances in atmospheric optics, like its future development, are related to the development and improvement of laser lidar systems for remote atmospheric probing. Used most extensively in the investigations of optical atmospheric characteristics and atmospheric aerosol are lidars designed on the basis of pulsed lasers [19, 78]. The following requirements are imposed on the transmitter of a lidar complex: (i) lasing at given wavelengths; (ii) stability of the pulse energy; (iii) a high laser efficiency. Exciplex lasers, which are the highest-power sources of pulsed UV radiation, satisfy all these requirements and in addition possess a relatively broad lasing spectrum, which can be regarded as an advantage in the solution of atmospheric monitoring problems by the technique of differential probing.

This is one of the most-employed techniques in the measurements of the atmospheric concentration of industrial pollutants (SO_2, NO_2) and ozone. It relies on the measurement of intensity difference of the radiation backscattered by a pollutant from the laser signals generated at two wavelengths. The greatest promise is exhibited by the lidars that allow conducting measurements for the greatest number of pollutants without significant changes of laser configuration. This is precisely the reason why the large spectral width of exciplex lasers gives them an edge on other lasers. On the one hand, modern techniques of spectral selection enable an easy extraction of a narrow emission line at the requisite wavelength and, on the other hand, the wavelength can be equally easy changed through its tuning across the emission spectrum. Furthermore, the power of exciplex lasers is high enough for the conversion of their radiation to other spectral regions by nonlinear optical techniques and also for pumping dye lasers [19, 78].

5.1 LIDA laser as a lidar for SO_2 concentration diagnostics

The LIDA type lasers were developed in the HCEI SB RAS as multi-purpose electric discharge lasers of the joule energy level [50, 52, 79]. In this case, the basic mixtures for these lasers are those with $XeCl^*$, XeF^*, $KrCl^*$, and KrF^* exciplex working molecules. We emphasise that after an insignificant modernisation these lasers can also be used to advantage as IR, UV, and visible radiation sources with HF, CO_2, N_2, etc. molecules. The XeCl laser is most extensively used for atmospheric probing, and therefore in the subsequent discussion we consider the LIDA laser operation at a wavelength of ~ 308 nm. The generalised design of one of these lasers is schematised in Fig. 19a.

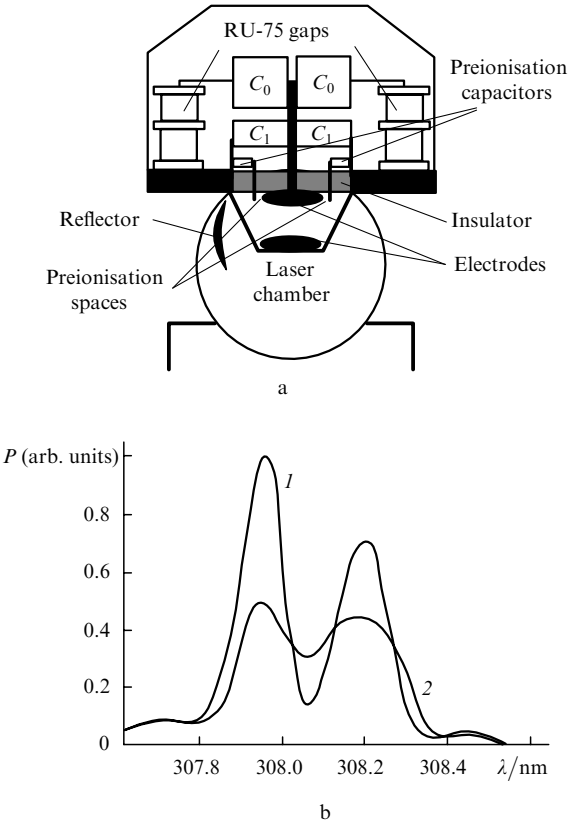

Figure 19. Schematic of the LIDA laser design (a) and structure of the output radiation spectrum of an electric discharge XeCl laser operated in the free running mode (*1*) and with enhanced relative intensity of the weak lines (*2*) (b).

In the free running mode, the XeCl laser emission spectrum consists of four lines corresponding to the $B-X$ electronic transitions. In this case, the $0-1$ and $0-2$ transition lines are commonly referred to as strong while the $0-0$ and $0-3$ transition lines as weak, since the intensities of the former lines in the spectrum exceed the intensities of the latter by an order of magnitude (Fig. 19b). This spectral structure has proved to be convenient for measuring the concentration of SO_2 molecules in the atmosphere. The $\lambda = 307.7$ nm (weak) line lies in the atmospheric transparency window (falls on the edge of absorption band of the SO_2 molecule), while the $\lambda = 308.45$ nm (strong) line falls on the centre of the same absorption band of the SO_2 molecule.

Also solved in the development of the differential lidar were the problems related primarily to the production of a narrow-band signal at the wavelength of the weak line, whose intensity should far exceed the intensity of the broadband noise developing from the spontaneous radiation at the wavelengths of the strong spectral lines. The production of a sufficiently intense signal in this case is possible only with the use of an oscillator–amplifier system. In Ref. [80] an investigation was made of the effect of pump parameters on the structure of the XeCl laser spectrum and the following requirements were formulated: the pump power density should exceed 1 MW cm^{-3} to provide a gain increment $gl > 6$ (here, g is the small-signal gain coefficient and l is the active length); the duration of the pump pulse should exceed the saturation times for the strong transitions, which amount to ~ 20 ns for typical laser parameters; the xenon density in the mixture should be 1.5–2 times greater than the density optimal from the viewpoint of output power maximisation.

The fulfilment of these conditions permits obtaining an output spectrum with enhanced relative intensities of the weak lines [Fig. 19b, curve (*2*)]. However, since the radiation at the strong lines nevertheless remains more intense, to efficiently extract the narrow weak line from the spectrum requires an optical resonator possessing, on the one hand, a high selectivity and minimal losses in the optical elements on the other. A schematic of such a resonator is diagrammed in Fig. 20. A diffraction grating (*1*) operates in the autocollimation mode here to provide a reflectivity of 0.7 in the first diffraction order, which is comparable with the reflectivity of an aluminium mirror. The spatial radiation selection is provided by a filter made up of a long-focus lens (*2*) ($F = 2$ m) and an aperture stop (*3*) with a diameter of 30–100 μm placed at its focus. Owing to a high radiation power density formed in the resonator, the output mirror (*5*) was displaced from the focus by 10 cm and placed behind a collimating lens (*4*). This resonator configuration permitted maximising the useful volume of the active laser medium ($3.5 \times 1.2 \times 60$ cm) and obtaining an energy of 3 mJ for a line width of 0.025 nm ($\lambda = 307.7$ nm) and 30 mJ for a line width of 0.04 nm ($\lambda = 308.45$ nm) at the oscillator output. In this case, the signal-to-noise ratio (the contrast ratio) was greater than 100 at a distance of 2 m from the output laser window. We note that the contrast ratio increased with the distance squared.

The LIDA laser was also employed as the amplifier of the narrow-band signal extracted. Two amplification modes were investigated: a single-pass mode and the mode of injection locking. In the latter case, the competition between the spontaneous noise at the wavelengths of the strong lines and the useful signal at the weak line in the amplifier medium is particularly critical. To maximise the contrast

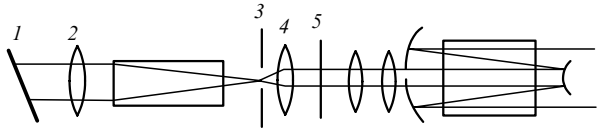

Figure 20. Optical scheme of the master oscillator and amplifier operating in the injection locking mode. The optical system was devised to obtain a high-power narrow-band high-contrast radiation at the wavelength of the weak line of the spectrum of the $XeCl^*$ molecule: (*1*) diffraction grating; (*2*) long-focus lens; (*3*) aperture; (*4*) lens; (*5*) resonator mirror.

ratio at the output in this case, the optimal delay between the switching of the oscillator and the amplifier should be equal to ~ 30 ns. This affords a signal-to-noise ratio of 5–10 at a distance of 2 m from the output amplifier mirror.

A radiation with a higher contrast ratio was obtained with the single-pass amplification mode. In this case, it was possible to raise the contrast ratio by selecting the geometry of radiation propagation in the amplifier and to obtain a contrast ratio of 100 in the amplification of a diverging beam. This mode was adopted as the mode best suited for the solution of the probing problem and enabled obtaining in the final version an energy of 120 mJ for a line width of 0.025 nm ($\lambda = 307.7$ nm) and 250 mJ for a line width of 0.04 nm ($\lambda = 308.45$ nm). The optimal delay between the oscillator switching and the amplifier switching was equal to 5–10 ns.

5.2 NO_2 diagnostics

The advent of high-power exciplex lasers was a powerful spur to the progress of high-power tunable dye lasers [19, 78]. Dye laser systems pumped by exciplex lasers are capable of generating radiation in the 430–550 nm range with an average power three times higher than that for similar systems pumped by Nd:YAG lasers [81]. Such systems find wide use, in particular, in the field of atmospheric probing. For instance, with their aid it is possible to solve the problem of determination of atmospheric NO_2 concentration, which is quite topical, particularly for megalopolises. To do this requires only two wavelengths: $\lambda = 446.9$ nm (at the centre of absorption band of the NO_2 molecule) and $\lambda = 448.2$ nm (the edge of absorption band of the NO_2 molecule). A narrow-band radiation at these wavelengths with a sufficiently high power (150 mJ, 0.01 nm) was generated with a high-power liquid dye laser (HPLL) utilising coumarin-2 [78]. The HPLL system, which was elaborated in the Laser Physics Laboratory of the Kuznetsov Siberian Physicotechnical Institute attached to the Tomsk State University, was designed specifically for pumping by the LIDA exciplex laser.

Using the LIDA lasers (an oscillator and an amplifier) and the HPLL system as the base, the Research and Production Association of Space Instrument Building (NPO KP, Moscow) developed a lidar complex for measuring the concentrations of the SO_2 and NO_2 pollutants. When measuring the SO_2 density, only the exciplex lasers were bound to operate. When measuring the NO_2 concentration, the radiation of the XeCl lasers was employed to pump the HPLL system. Since 1997, this lidar complex has been used to advantage by the NPO KP for NO_2 monitoring in the Moscow air basin [78].

6. Conclusions

Therefore, important results were obtained in the investigation and development of pulsed dense-gas lasers as well as with by using these lasers owing to Academician A.M. Prokhorov's support and the cooperation between the scientific bodies of the HCEI SB RAS and the GPI RAS during the 1970s-90s.

Acknowledgements. The authors wish to express their deep gratitude to the HCEI SB RAS and GPI RAS staff members who were participants and co-authors of Refs [1–38].

References

1. Bugaev S.P., Bychkov Yu.I., Karlova E.K., Karlov N.V., Koval'chuk B.M., Kuz'min G.P., Kurbatov Yu.A., Mesyats G.A., Orlovskii V.M., Prokhorov A.M., Rybalov A.M. *Pis'ma Zh. Tekh. Fiz*., **1**, 492 (1975).
2. Bychkov Yu.I., Karlova E.K., Karlov N.V., Koval'chuk B.M., Kuz'min G.P., Kurbatov Yu.A., Mesyats G.A., Orlovskii V.M., Prokhorov A.M., Rybalov A.M. *Pis'ma Zh. Tekh. Fiz*., **2**, 212 (1976).
3. Bychkov Yu.I., Zagulov F.Ya., Karlov N.V., Kovsharov N.F., Losev V.F., Mesyats G.A., Prokhorov A.M., Tarasenko V.F. *Pis'ma Zh. Tekh. Fiz*., **2**, 1052 (1976).
4. Datskevich N.P., Karlova E.K., Karlov N.V., Koval'chuk B.M., Konev Yu.B., Kononov N.N., Kochetov I.V., Kuz'min G.P., Mesyats G.A., Nikiforov S.M., Pevgov V.G., Prokhorov A.M. *Kvantovaya Elektron*., **4**, 457 (1977) [*Sov. J. Quantum Electron*., **7**, 258 (1977)].
5. Bychkov Yu.I., Karlov N.V., Konovalov I.N., Mesyats G.A., Prokhorov A.M., Tarasenko V.F. *Pis'ma Zh. Tekh. Fiz*., **3**, 1041 (1977).
6. Bychkov Yu.I., Karlov N.V., Losev V.F., Mesyats G.A., Prokhorov A.M., Tarasenko V.F. *Pis'ma Zh. Tekh. Fiz*., **4**, 83 (1978).
7. Alimpiev S.S., Bychkov Yu.I., Karlov N.V., Karlova E.K., Mesyats G.A., Nabiev M.Sh., Nikiforov S.M., Orlovskii V.M., Osipov V.V., Prokhorov A.M., Khokhlov E.M. *Pis'ma Zh. Tekh. Fiz*., **5**, 816 (1979).
8. Alimpiev S.S., Karlov N.V., Mesyats G.A., Nikiforov S.M., Orlovskii V.M., Prokhorov A.M., Sartakov B.G., Khokhlov E.M., Shtarkov A.A. *Pis'ma Zh. Eksp. Teor. Fiz*., **30**, 279 (1979).
9. Bychkov Yu.I., Konovalov I.N., Losev V.F., Mesyats G.A., Prokhorov A.M., Sisakyan I.N., Tarasenko V.F., Filonov A.G. *Pis'ma Zh. Tekh. Fiz*., **6**, 1483 (1980).
10. Apollonov V.V., Bunkin V.F., Bychkov Yu.I., Konovalov I.N., Losev V.F., Mesyats G.A., Prokhorov A.M., Tarasenko V.F., Firsov K.N. *Kvantovaya Elektron*., **8**, 1331 (1981) [*Sov. J. Quantum Electron*., **11**, 798 (1981)].
11. Apollonov V.V., Bunkin V.F., Bychkov Yu.I., Konovalov I.N., Losev V.F., Mesyats G.A., Prokhorov A.M., Tarasenko V.F., Firsov K.N., Chesnokov S.M. *Izv. Akad. Nauk SSSR, Ser. Fiz*., **45**, 989 (1981).
12. Ageev V.P., Gorbunov A.A., Konov V.I., Lukovnikov D.S., Mel'chenko S.V., Prokhorov A.M., Tarasenko V.F. *Kvantovaya Elektron*., **10**, 1466 (1983) [*Sov. J. Quantum Electron*., **13**, 954 (1983)].
13. Bychkov Yu.I., Zaroslov D.Yu., Karlov N.V., Kuz'min G.P., Mesyats G.A., Osipov V.V., Prokhorov A.M., Tel'nov V.A. *Kvantovaya Elektron*., **9**, 1718 (1982) [*Sov. J. Quantum Electron*., **12**, 1105 (1982)].
14. Bychkov Yu.I., Zaroslov D.Yu., Karlov N.V., Kuz'min G.P., Mesyats G.A., Osipov V.V., Prokhorov A.M., Tel'nov V.A. *Zh. Tekh. Fiz*., **53**, 1489 (1983).
15. Bychkov Yu.I., Zaroslov D.Yu., Karlov N.V., Kuz'min G.P., Mesyats G.A., Osipov V.V., Prokhorov A.M., Tel'nov V.A. *Zh. Tekh. Fiz*., **53**, 2138 (1983).
16. Genkin S.A., Karlov N.V., Klimenko K.A., Korolev Yu.D., Kuz'min G.P., Mesyats G.A., Novoselov Yu.N., Prokhorov A.M. *Pis'ma Zh. Tekh. Fiz*., **10**, 641 (1984).
17. Kozyrev A.V., Korolev Yu.D., Mesyats G.A., Novoselov Yu.N., Prokhorov A.M., Skakun V.S., Tarasenko V.F., Genkin S.A. *Kvantovaya Elektron*., **11**, 524 (1984) [*Sov. J. Quantum Electron*., **14**, 356 (1984)].
18. Derzhiev V.I., Koval' N.N., Mesyats G.A., Prokhorov A.M., Skakun V.S., Tarasenko V.F., Tolkachev V.S., Fomin E.A., Yakovlenko S.I. *Kvantovaya Elektron*., **14**, 427 (1987) [*Sov. J. Quantum Electron*., **17**, 269 (1987)].
19. Gochelashvili K.S., Kabanov M.V., Kaul' V.B., Kopylova T.N., Maier G.V., Mel'chenko S.V., Panchenko A.N., Prokhorov A.M., Tarasenko V.F., Tel'minov E.N. *Laser Phys*., **2**, 802 (1992).
20. Bunkin F.V., Derzhiev V.I., Mesyats G.A., Skakun V.S., Tarasenko V.F., Yurovskii V.A., Yakovlenko S.I. *Kvantovaya Elektron*., **11**, 1277 (1984) [*Sov. J. Quantum Electron*., **14**, 864 (1984)].

21. Zaroslov D.Yu., Kuz'min G.P., Tarasenko V.F. *Radiotekh. Elektron.*, **24**, 1217 (1984).
22. Bunkin F.V., Derzhiev V.I., Mesyats G.A., Skakun V.S., Tarasenko V.F., Yakovlenko S.I. *Kvantovaya Elektron.*, **12**, 245 (1985) [*Sov. J. Quantum Electron.*, **15**, 159 (1985)].
23. Bunkin F.V., Derzhiev V.I., Mesyats G.A., Skakun V.S., Tarasenko V.F., Yakovlenko S.I. *Kvantovaya Elektron.*, **12**, 874 (1985) [*Sov. J. Quantum Electron.*, **15**, 575 (1985)].
24. Bunkin F.V., Derzhiev V.I., Mesyats G.A., Skakun V.S., Tarasenko V.F., Fedenev A.V., Yakovlenko S.I. *Kvantovaya Elektron.*, **12**, 1993 (1985) [*Sov. J. Quantum Electron.*, **15**, 1316 (1985)].
25. Derzhiev V.I., Losev V.F., Skakun V.S., Tarasenko V.F., Yakovlenko S.I. *Opt. Spektrosk.*, **60**, 811 (1986).
26. Bunkin F.V., Derzhiev V.I., Mesyats G.A., Murav'ev I.I., Skakun V.S., Tarasenko V.F., Fedenev A.V., Yakovlenko S.I., Yancharina A.M. *Izv. Akad. Nauk SSSR, Ser. Fiz.*, **50**, 1064 (1986).
27. Bunkin F.V., Datskevich N.P., Derzhiev V.I., Karlov N.V., Kuz'min G.P., Mesyats G.A., Skakun V.S., Tarasenko V.F., Yakovlenko S.I. *Kvantovaya Elektron.*, **13**, 878 (1986) [*Sov. J. Quantum Electron.*, **16**, 576 (1986)].
28. Bunkin F.V., Derzhiev V.I., Mesyats G.A., Skakun V.S., Tarasenko V.F., Shpak V.G., Yakovlenko S.I. *Zh. Tekh. Fiz.*, **56**, 2240 (1986).
29. Bunkin F.V., Derzhiev V.I., Koval' N.N., Mesyats G.A., Skakun V.S., Tarasenko V.F., Shchanin P.M., Yakovlenko S.I. *Radiotekh. Elektron.*, **32**, 1672 (1987).
30. Bunkin F.V., Derzhiev V.T., Mesyats G.A., Skakun V.S., Tarasenko V.F., Yakovlenko S.I. *J. Opt. Soc. Am.*, **3**, 989 (1986).
31. Sereda O.V., Tarasenko V.F., Fedenev A.V., Yakovlenko S.I. *Kvantovaya Elektron.*, **20**, 535 (1993) [*Quantum Electron.*, **23**, 459 (1993)].
32. Boichenko A.M., Tarasenko V.F., Fomin E.A., Yakovlenko S.I. *Kvantovaya Elektron.*, **20**, 7 (1993) [*Quantum Electron.*, **23**, 3 (1993)].
33. Tarasenko V.F., Yakovlenko S.I. *Kvantovaya Elektron.*, **24**, 1145 (1997) [*Quantum Electron.*, **27**, 1111 (1997)].
34. Karelin A.V., Tarasenko V.F., Yakovlenko S.I. *Laser Phys.*, **10**, 827 (2000).
35. Boichenko A.M., Tarasenko V.F., Yakovlenko S.I. *Laser Phys.*, **10**, 1157 (2000).
36. Bychkov Yu.I., Koval'chuk B.M., Kuz'min G.P., Mesyats G.A., Tarasenko V.F. *Izv. Vyssh. Uchebn. Zaved., Ser. Fiz.*, (5), 5 (2000).
37. Boichenko A.M., Skakun V.S., Sosnin E.A., Tarasenko V.F., Yakovlenko S.I. *Laser Phys.*, **10**, 540 (2000).
38. Arnold E., Lomaev M.I., Skakun V.S., Tarasenko V.F., Tkachev A.N., Shitts D.V., Yakovlenko S.I. *Laser Phys.*, **12**, 1270 (2002).
39. *Gazovye lazery* (Gas Lasers) N.N. Sobolev (Ed.), with contributions from Bennett W.R. Jr., Gould G., Bloom A.L., etc. (Moscow: Mir, 1968).
40. Allen L., Jones D. *Principles of Gas Lasers* (London: Butterworths, 1967).
41. Gudzenko L.I., Yakovlenko S.I. *Plazmennye lazery* (Plasma Lasers) (Moscow: Atomizdat, 1978).
42. Prokhorov A.M. (Ed.) *Spravochnik po lazeram* (Handbook of Lasers) (Moscow: Sov. Radio, 1978) Vol. 1.
43. Prokhorov A.M. (Ed.) *Spravochnik po lazeram* (Handbook of Lasers) (Moscow: Sov. Radio, 1978) Vol. 2.
44. Rhodes C.K. (Ed.) *Excimer Lasers* (New York: Springer-Verlag, 1979).
45. Basov N.G. (Ed.) *Khimicheskie lazery* (Chemical Lasers) (Moscow: Nauka, 1982).
46. Svelto O. *Principles of Lasers* (New York: Plenum Press, 1982).
47. McDaniel E.W., Nigan W. (Eds) *Applied Atomic Collision Physics* (New York: Academic Press, 1982) Vol. 3.
48. Baranov V.Yu., Borisov B.M., Stepanov Yu.Yu. *Elektrorazryadnye eksimernye lazery na galogenidakh inertnykh gazov* (Electric Discharge Excimer Lasers Utilising Rare-Gas Halides) (Moscow: Energoatomizdat, 1988).
49. Aleinikov V.S., Masychev V.I. *Lazery na okisi ugleroda* (Carbon Monoxide Lasers) (Moscow: Radio i Svyaz', 1990).
50. Mesyats G.A., Osipov V.V., Tarasenko V.F. *Impul'snye gazovye lazery* (Pulsed Gas Lasers) (Moscow: Nauka, 1991).
51. Donin V.I. *Moshchnye ionnye gazovye lazery* (High-Power Ion Gas Lasers) (Novosibirsk: Nauka, 1991).
52. Mesyats G.A., Osipov V.V., Tarasenko V.F. *Pulsed Gas Lasers* (Washington: SPIE Press, 1995).
53. Molchanov A.G. *Usp. Fiz. Nauk*, **106**, 165 (1972).
54. Gudzenko L.I., Shelepin L.A., Yakovlenko S.I. *Usp. Fiz. Nauk*, **114**, 457 (1974).
55. Rodes C.K. *IEEE J. Quantum Electron.*, **10** (12), 153 (1977).
56. Koval'chuk B.M., Kremnev V.V., Mesyats G.A. *Dokl. Akad. Nauk SSSR*, **191**, 76 (1970).
57. Basov N.G., Belenov E.M., Danilychev V.A., Suchkov A.F., in *Kvantovaya Elektron.*, (3), 121 (1971) [*Sov. J. Quantum Electron.*, **1** (3), 306 (1971)].
58. Fenstenmaher C.A., Hufter M.I., Rink I.P., Boyer K. *Bull. Am. Phys. Soc.*, (16), 42 (1971).
59. Basov N.G., Danilychev V.A., Ionin A.A., Kovsh I.B., Sobolev V.A. *Zh. Tekh. Fiz.*, **43**, 2357 (1973).
60. Cason C., Dezenberg G., Huff R.J. *Appl. Phys. Lett.*, **23**, 110 (1973).
61. Anisimov V.N., Baranov V.Yu., Borzenko V.L., et al. *Kvantovaya Elektron.*, **7**, 1451 (1980) [*Sov. J. Quantum Electron.*, **10**, 835 (1980)].
62. Yamanaka C., Nakai S., Matova M. *IEEE J. Quantum Electron.*, **17**, 1678 (1981).
63. Carlson R.L., Carpenter J.P., Casperson D.E., et al. *IEEE J. Quantum Electron.*, **17**, 1662 (1981).
64. Mesyats G.A. (Ed.) *Razrabotka i primenenie istochnikov intensivnykh elektronnykh puchkov* (Development and Application of Intense Electron Beam Sources) (Novosibirsk: Nauka, 1976).
65. Mesyats G.A. (Ed.) *Sil'notochnye impul'snye elektronnye puchki v tekhnologii* (High-Current Pulsed Electron Beams in Technology) (Novosibirsk: Nauka, 1983).
66. Bychkov Yu.I., Orlovskii V.M., Osipov V.V. *Kvantovaya Elektron.*, **4**, 2435 (1977) [*Sov. J. Quantum Electron.*, **7**, 1390 (1977)].
67. Bychkov Yu.I., Losev V.F., Mesyats G.A., Tarasenko V.F. *Kvantovaya Elektron.*, **4**, 1385 (1977) [*Sov. J. Quantum Electron.*, **7**, 789 (1977)].
68. Bychkov Yu.I., Korolev Yu.D., Losev V.F., Tarasenko V.F., Khuzeev A.P., Shemyakin I.A. *Izv. Vyssh. Uchebn. Zaved., Ser. Fiz.*, (12), 57 (1977).
69. Bychkov Yu.I., Losev V.F., Savin V.V., Tarasenko V.F. *Izv. Vyssh. Uchebn. Zaved., Ser. Fiz.*, (1), 81 (1978).
70. Tarasenko V.F., Baksht E.H., Fedenev A.V., Orlovskii V.M., Panchenko A.N., Skakun V.S., Sosnin E.A. *Proc. SPIE. Int. Soc. Opt. Eng.*, **3343**, 715 (1998).
71. Bychkov Yu.I., Losev V.F., Mesyats G.A., Tarasenko V.F. *Pis'ma Zh. Tekh. Fiz.*, **3**, 1223 (1977).
72. Searles S.K., Hart G.A. *Appl. Phys. Lett.*, **27**, 243 (1975).
73. Ewing J.J., Brau C.A. *Appl. Phys. Lett.*, **27**, 350 (1975).
74. Ault E.R., Branford R.S., Bhaumik M.L. *Appl. Phys. Lett.*, **27**, 413 (1975).
75. Bychkov Yu.I., Ivanov N.G., Konovalov I.N., Losev V.F., Tarasenko V.F., Tel'minov E.N. *Kvantovaya Elektron.*, **10**, 1510 (1983) [*Sov. J. Quantum Electron.*, **13**, 990 (1983)].
76. Abdullin E.N., Gorbachev S.I., Efremov A.I., Koval'chuk B.M., Loginov S.V., Skakun V.S., Tarasenko V.F., Tolkachev V.S., Fedenev A.V., Fomin E.A., Shchanin P.M. *Kvantovaya Elektron.*, **20**, 652 (1993) [*Quantum Electron.*, **23**, 564 (1993)].
77. Koval'chuk B.M., Losev V.F., Mesyats G.A., Tarasenko V.F. *Izv. Vyssh. Uchebn. Zaved., Ser. Fiz.*, (5), 12 (2000).
78. Tarasenko V.F., Baksht E.H., Kopylova T.N., Kunts S.E., Kuznetsova R.T., Maier G.V., Mel'chenko S.V., Onitschenko A.L., Panchenko A.N., Samsonova L.G., Svetlichnyi V.A., Tel'minov E.N. *Proc. Conf. Lasers'98* (McLEAN: STS Press, 1999) p. 525.
79. Mel'chenko S.V., Panchenko A.N., Tarasenko V.F. *Pis'ma Zh. Tekh. Fiz.*, **12**, 171 (1986).
80. Kaul' V.B., Kunts S.E., Mel'chenko S.V. *Kvantovaya Elektron.*, **22**, 555 (1995) [*Quantum Electron.*, **25**, 529 (1995)].
81. Artykhov V.Ya., Sokolova I.V., Kopylova T.N., Maier G.V., Tarasenko V.F. *Proc. Conf. Lasers'94* (McLEAN: STS Press, 1995) p. 208.